

Multispectral Recognition Using Genetic and Evolutionary Feature Extraction

Pablo A. Arias, Joseph Shelton, Kaushik Roy, Gerry V. Dozier, Foysal Ahmad

Department of Computer Science, North Carolina A&T State University, Greensboro, U.S.A

Center for Advanced Studies in Identity Sciences @ NC A&T

{parias, jashelt1, fahmad}@aggies.ncat.edu, {kroy, gvdozier}@ncat.edu

Abstract

Traditionally, iris recognition systems capture iris images in the 700 to 900nm range. It is within these ranges that researchers have found the most viable iris textures for iris recognition. Recently, there has been an interest for exploration of spectrum ranges that falls outside of these traditional ranges. In this work, we will explore the performance of feature extraction techniques on a wider spectrum, specifically ranges between 400nm to 1550nm. More specifically, we apply the traditional Local Binary Pattern (LBP) technique & a hybrid LBP technique (Genetic and Evolutionary Feature Extraction (GEFE)) in an effort to elicit the most important iris information. We also perform intra-spectral and cross spectrum analysis on the iris images captured in different wavelengths. Results show that GEFE outperforms the LBP technique on all spectrums.

Introduction

Biometric technologies are becoming the predominate form of access control. Physiological and behavioral traits are aspects of biometrics that allows for unique forms of identification. The physiological traits (face, iris, fingerprint, etc.) have many advantages over the traditional techniques such as knowledge and/or token based access control. Knowledge can be forgotten and tokens can be easily stolen, whereas physiological traits cannot be forgotten or easily stolen. Biometrics is a subarea of the broader field of identity science. "Identity Science is the field of study devoted towards the understanding of how the dynamic nature of 'self' interacts with a possibly intractable number of dynamic environments in an effort to observe, track, and identify 'self' (in terms of its beliefs, desires, intentions, regression, progression, etc.) via a set of external witnesses. (Dozier 2015)". An external witness can be viewed as any entity that has the ability to: perceive an interaction between 'self' and an environment, process the observed interaction, and track and/or identify 'self' with respect to that environment.

The iris biometric has been shown to be a viable biometric for verification and identification (Ross 2010,

Masek 2003). Daugman developed the first iris recognition algorithm (Daugman 2004), and many researchers have further extended the work of iris recognition (Verma et al. 2012, Bowyer, Hollingsworth and Flynn 2008, Sanchez-Avila and Sanchez-Reillo 2005). Google headquarters uses iris recognition access control systems for identifying individuals (Adam, Neven and Steffens 2010), and the company M2SYS Technology has patented an iris identification system that can link hospital patients to their medical records (Archbold 2014). In the Penobscot Country Jail, iris scanners are being implemented in order to eliminate improper inmate releases (Ricker 2006).

The iris biometric has advantages over other types of biometrics. The accuracy of recognition is generally better than the accuracy of other biometrics such as facial or fingerprint (Masek 2003). An iris is also well protected by wear and tear, as opposed to one's fingerprint. There are disadvantages in that the iris is small and intricate, which makes it difficult to obtain from any significant distance without missing vital information. Individuals who may have eye issues such as blindness or cataracts could also be difficult to recognize. Environmental issues can also be a factor in regards to poor lighting or shade. Finally, the iris can often be covered by eyewear such as glasses or shades.

Images captured in the near infrared (NIR) wavelength band contains more iris textural information than images captured in the visible wavelength. Most of the current iris recognition schemes capture iris images in the NIR wavelength band. This range is generally from 700nm to 900nm. Though iris recognition using NIR wavelengths has an acceptable recognition rate, there are still vulnerabilities such as faking iris images (Park and Kang 2005). Researchers are interested in exploring the wavelengths outside of the 700nm-900nm range.

Most of the existing multispectral iris recognition systems use Gabor filters as a feature extraction technique (Daugman 2004). There has been research done using texture based feature extraction methods such as a Modified Local Binary Pattern (MLBP) algorithm (Poplewell et al. 2014). This variation of the Local Binary Pattern (LBP) algorithm (Shelton et al. 2011) segments an

image into even sized regions and extracts features from each region. Each region can be referred to as a patch. MLBP segments a biometric image into sub-regions and extracts more features from each patch than traditional LBP. A Cooperative Game Theory (CGT) based patch selector was implemented in (Ahmad, Roy and Popplewell 2014). Though the CGT with MLBP method showed promise, the approach reported in (Ahmad, Roy and Popplewell 2014) utilized only the patches based on the image partition of LBP. It is possible that noisy data may be included if patches from the entire image space are considered. To mitigate this, we propose the application of a genetic algorithm-based feature extraction technique. This feature extraction method evolves Feature Extractors (FEs) that can have patches of varying sizes in various positions on an image and applies them in an overlapping fashion.

In the past, a feature extraction technique known as Genetic and Evolutionary Feature Extraction (GEFE) was created at the Center for Advance Studies in Identity Science (CASIS) (Shelton et al. 2011, Shelton et al. 2014). GEFE was initially applied on facial images (Shelton et al. 2011) but has been recently applied on iris images (Shelton et al. 2014).

GEFE is an instance of a Genetic and Evolutionary Computation (GEC), an algorithm that uses natural selection techniques to evolve a population of candidate solutions for a problem (Engelbracht 2007, Davis 1991, Goldberg 1989). GEFE would allow sub-regions to be any location on an image and to be any size. Previous research has shown success of GEFE when testing on a single modality; GEFE outperformed traditional LBP in terms of recognition accuracy as well as the number of features used. In this work, we will apply GEFE towards multispectral iris recognition (O'Connor et al. 2014). More specifically, we will conduct inter-spectral and cross-spectral recognition on a wide range of spectrums (450nm-1550nm) to determine the effectiveness of GEFE on this dataset.

The remainder of this paper is as follows. In Section 2, we will discuss the feature extraction methods used. In Section 3, we will describe the experimental setup. Section 4 will contain the results of the experiments and Section 5 provides the conclusions and future remarks.

Feature Extraction Methods

Local Binary Patterns

The Local Binary Pattern (LBP) feature extraction algorithm is a method that is used for texture classification (Ojala, Pietikainen and Maenpaa 2002, Ahonen, Hadid and Pietikainen 2006). This technique can be used to classify textures patterns in images and it uses these textures to create Feature Vectors (FVs) for images. For biometric recognition, the LBP technique works by

segmenting an image into uniform sized, non-overlapping regions, as shown in Figure 1. Each region has a histogram associated with it, where the bins in the histogram correspond to the texture patterns found in each region. A FV is created by concatenating the histograms from all regions of a segmented image.

Texture patterns are created by comparing center pixels, a pixel that is surrounded by i number of neighboring pixels on all sides, with the i neighboring pixels. A texture pattern can be represented as a binary string, and that string can be decoded into a decimal value, denoted as $LBP(N_i, c)$, where c is the pixel intensity value of a center pixel, N is a set of neighboring pixel intensity values and i is the i^{th} neighboring pixel of c . $LBP(N_i, c)$ is computed in (1) and (2), where the difference is taken between each neighboring pixel and a center pixel. The equation $s(N_i, c)$ computes the difference and returns the appropriate bit.

$$LBP(N_i, c) = \sum_{i=0}^{i-1} s(N_i, c) 2^i \quad (1)$$

$$s(N_i, c) = \begin{cases} 0, & \text{if } N_i - c < 0 \\ 1, & \text{if } N_i - c \geq 0 \end{cases} \quad (2)$$

The total number of texture patterns that can exist depend on the number of neighboring pixels, i , where the number of possible patterns are 2^i . However, the common way to create FVs with the LBP technique is to use mostly uniform patterns for bins in the histograms. A uniform pattern is one where the bit transitions in a texture pattern changes two or fewer times when traversing the texture pattern circularly.

The common variation of the LBP technique is popular, but it is also possible to simply consider all of the possible patterns as opposed to just uniform patterns. In this case, histograms would be length 2^i , or, for a neighborhood size of 8, $2^8 = 256$.

During the process of recognition, a probe template, p , is compared to a gallery set of vectors $G = \{g_0, g_1, \dots, g_{k-1}\}$ using the (Manhattan) City Block distance metric. This distance is a numerical representation of the distinction between two biometric instances and can be calculated using the following formula:

$$d = \sum_{i=0}^n |p_i - g_{k,i}| \quad (3)$$

where d is the distance between two subjects, p is the probe feature template, g is the gallery feature template in set G , n is total number of features, i is the index of the feature, and k is the k^{th} individual in the gallery. The subject, g_k , is considered a match to p when distance between the two vectors is the smallest compared to all other subjects in G .

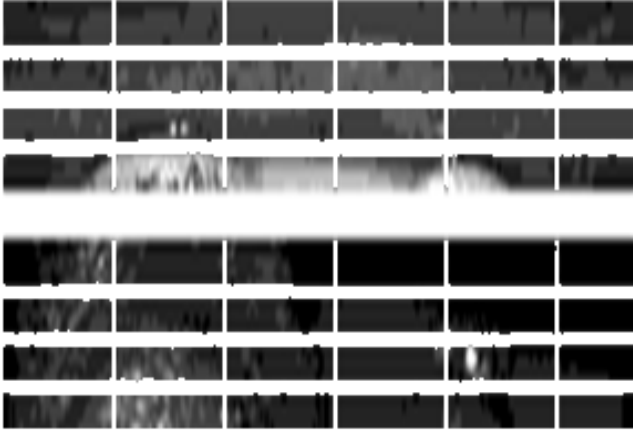


Figure 1: Image partitioned into patches

GEFEML

GEFE is an instance of a GEC that evolves LBP-based FEs. Whereas a traditional LBP FE uses even sized, non-overlapping patches over an entire image, GEFE evolves FEs that can have patches of varying sizes in various positions on an image. Because GEFE is an instance of a GEC, a FE must be represented as a candidate solution. We use a 6-tuple with 5 sets and 1 single value, represented as $\langle X_i, Y_i, W_i, H_i, M_i, f_i \rangle$. Each of the patches in a particular FE, fe_i , are designed using the values in the 6-tuple. The X_i and Y_i sets hold the $\langle X, Y \rangle$ points of the center of each patch in fe_i , while the sets W_i and H_i holds the width and heights of the patches. The set M_i denotes a masking value for each patch in fe_i . Though there can be multiple patches defined by the 6-tuple, a patch's specific masking value determines whether the features extracted by that patch are included in the resulting FV.

The fitness, f_i , is determined by applying fe_i towards a dataset of subject's iris images. A subject has a number of images that vary, and these images are separated into a probe set and a gallery set (G). The fe_i is applied on these images to create FVs, and the FVs in the probe set are compared to all of the FVs in the gallery set using the Manhattan distance measure. The two FVs that have the least Manhattan distance are considered to be matches. If a probe FV is incorrectly matched with a gallery FV, then fe_i is said to cause an error. The resulting f_i is the number of errors (ϵ) added to the percent of patches not masked out (ζ), shown below.

$$f_i = 10\epsilon + \zeta \quad (4)$$

Previous research in (Shelton et al. 2011) has shown that GEFE instances with uniform patch sizes had a statistically better performance than GEFE instances with non-uniform patches. This means that the sets W_i and H_i will have one value in their set, representing the parameters for all patches in fe_i .

In the original implementation of GEFE, a set of FEs were evolved on a training set to produce FEs that could correctly identify subjects in that particular data set. To produce FEs that could generalize well on unseen subjects, supervised learning was added to the GEFE process. Cross validation in Genetic and Evolutionary Feature Extraction – Machine Learning (GEFEML) (Shelton et al. 2012) is done by initially generating a population of random FEs. Every candidate FE is then evaluated on the training set and additionally evaluated on a validation set. The results of the FEs on the validation set do not affect the training of FEs. While a stopping condition has not been met, FEs are selected to breed, and offspring FEs are created. The offspring are evaluated on the training set, but they are also applied on the validation set. The FE with the best results on the validation set is stored as FE*. FE* is only updated when a new candidate FE performs better on the validation set than the currently stored FE*. The offspring are used to create the new population and this process repeats until the stopping condition has been met. Under this design, FE* should generalize better on unseen subjects opposed to the best performing FE on the training set.

Experiments

We conducted our experiments on a multispectral iris image dataset that contains 38,129 images (Multispectral Iris Dataset). These images were acquired using Goodrich/Sensors with a custom designed lens package to acquire iris images at wavelengths in the range 400 to 1600nm. We segmented the multispectral iris images using Canny edge detections in an effort to identify the iris regions and applied circular Hough transforms to define the iris and pupil boundaries (Masek 2003, Popplewell et al. 2014). A technique based on Daugman's Rubber Sheet Model was then used for normalization. These images were divided into 13 sections, each section depicting a spectral band consisting of roughly 2945 iris images. For our first experiment, we did intra-class comparisons for each spectral band. We divided the data set into three sections: training, validation, and testing. The training set had a total of 44 subjects, the validation set had 18 subjects, and the testing set had 29 subjects. We further separated each set into a probe set and a gallery set; the first sample of each subject went into the probe set while the remaining went into the gallery set. For GEFE, we ran it for 30 runs and for each run, we ran it for 1000 generations. For cross spectral analysis, we used features extractors evolved from intra-spectral comparisons and applied them to each of the differing spectral band images.

In this work, similarity scores are computed by modifying the Manhattan city block distance metric. The variables h_i and h_j represents two FVs being measured, l represents the length of the FV, and z represents the current position in the FV.

LBP and found that 7 columns by 10 rows was the best

performing partition. This 70 patch LBP partition is compared to GEFE in the results. Figures 2-5 show the normalized iris regions with the overlapped patches.

Results and Discussions

Shown in Table I are the test set accuracies of FE produced by different feature extraction algorithms. In the table, Spectrum represents the spectrum used for feature extraction on the training and validation set. For the Cross Spectrum, this represents the spectrum used for the test set. Accuracy represents the identification accuracy of the algorithm on the test set. For LBP, the number represents the accuracy of the traditional LBP feature extractor that partitions an image into 7 by 10. For the GEFE variations on the iris, GEFE <Opt> represents FEs that were optimized on the training set, while GEFE <Val> represents the best performing FEs on the validation set. For GEFE, the number on the outside represents the accuracy of the best feature extractor, whereas the number within the parenthesis represents the average accuracy of the 30 best FEs. The column P represents the number of patches used on average by the feature extractors.

Table I. Performance on multispectral iris dataset.

Spectrum	Cross Spectrum	Accuracy			Patches	
		LBP	GEFE		Opt	Val
			<Opt>	<Val>		
405	405	7.02	13.79(8.05)	12.07(6.21)	28.16	22.87
	800	n/a	96.55(89.83)	94.83(84.02)	28.16	22.87
505	505	45.61	63.79(53.79)	53.44(41.03)	32.80	24.15
	800	n/a	94.83(92.59)	96.55(86.09)	32.80	24.15
620	620	64.91	79.31(74.02)	74.13(60.80)	33.71	24.25
	1200	n/a	98.28(92.01)	93.10(81.49)	33.71	24.25
700	700	50.87	67.24(59.31)	63.79(56.84)	30.96	24.48
	800	n/a	96.55(93.62)	94.83(8.91)	30.96	24.48
800	800	91.23	98.28(94.54)	98.28(87.07)	28.76	24.71
	911	n/a	98.28(91.38)	94.83(84.26)	28.76	24.71
910	910	89.66	96.55(92.18)	96.55(84.37)	31.48	25.08
	800	n/a	96.55(87.30)	96.55(87.30)	25.08	25.08
911	911	87.93	96.55(90.75)	93.10(81.72)	31.22	24.88
	800	n/a	98.27(94.60)	96.55(86.32)	31.22	24.88
970	970	84.48	89.66(85.17)	87.93(75.46)	30.83	24.12
	800	n/a	98.28(94.60)	94.83(85.46)	30.83	24.12
1070	1070	89.66	94.83(89.31)	93.10(77.24)	30.92	25.08
	800	n/a	98.28(95.11)	96.55(87.99)	30.92	25.08
1200	1200	93.10	98.27(92.36)	93.10(78.79)	31.62	24.78
	800	n/a	98.28(94.66)	94.83(85.75)	31.62	24.78
1300	1300	82.76	93.10(89.66)	91.38(77.99)	33.59	25.27
	800	n/a	96.55(93.39)	94.83(85.00)	33.59	25.27
1450	1450	36.21	67.24(58.16)	51.72(31.72)	38.55	25.08
	911	n/a	98.28(92.76)	64.83(80.11)	38.55	25.08
1550	1550	31.03	43.10(36.94)	37.93(24.60)	34.15	24.71
	800	n/a	96.55(92.01)	96.55(86.49)	34.15	24.71

Results show that for all spectrums, GEFE outperforms traditional LBP within their respective spectrums ‘GEFE <Opt>’ and ‘GEFE <Val>’ had similar performances in respect to recognition accuracy, but with respect to the number of patches, GEFE <Opt> was proven to be statistically better. The results show that on average, the 800 nm spectrum performs the best for identification accuracy for both intra-class comparisons and cross spectrum comparisons. An ANOVA test was used as a statistical measure of performance, with a 95% confidence interval.

In Figures 2-5, the images show the best performing FEs on the 800nm test set. In Figures 2 and 3, the best opt-gen and val-gen FEs are shown. The areas with overlapping patches are the most salient areas to extract features from for identification. Figures 4 and 5 show the best cross-spectral FEs on the 800nm test set for opt-gen and val-gen. It appears that the right most area of iris images contains more salient texture information than the left area. Depending on if an iris is a left or right eye; there will be slight noisy data in the form of eyelashes. It could be the case that the grouping of patches on the right side is locking on to that noisy data or lack of. In Figures 6-9, we show the Cumulative Match Characteristic (CMC) curves and the Receiver Operator Characteristic (ROC) curves for LBP and the best FE from GEFE. The CMC curve plots the rank accuracies of the methods, while the ROC curve plots the True Accept Rate (TAR) and the False Accept Rate (FAR) of subjects. The results in Table 1 show that the 800 nm spectrum achieved rank 1 accuracy of 98.28% for both the opt-gen and val-gen FEs on the test set.



Figure 2: 800nm FE(Opt Gen) on 800nm Image.



Figure 3: 800nm FE (Val Gen) on 800nm Image.



Figure 4: 1070nm FE (Opt Gen) on 800nm Image.



Figure 5: 1070nm FE (Val Gen) on 800nm Image.

The CMC curves plot the accuracy at each rank. The rank represents the ranking of match scores for all probe subjects. For Figure 6 and 7, the ROC curve plots the rate of impostor attempts accepted on the x-axis, against the corresponding rate of genuine attempts accepted on the y-axis along an increasing threshold. In Figure 8, the CMC curves show a superior performance of GEFE compared to LBP. Though both techniques do not achieve 100% accuracy until rank 57, GEFE continues to outperform LBP. In Figure 9, the CMC curves for cross spectrum analysis were created by taking the best performing FEs from each spectrum when used for cross validation. It appears that the FE from the 800nm spectrum performed best in cross spectrum analysis. This supports the intra-class results, where the FEs on the 800nm spectrum had the best performance overall.

Even though the results show that FEs evolved on the 800 nm spectrum had the overall best performance, it is worth mentioning that some bands outside of the NIR range performed well. In Table 1, the performance of GEFE on the 620nm spectrum performed better than the 700nm spectrum not only in intra-class matching, but also using feature extractors from the 1200 nm spectrum. The performance of the 1200 nm feature extractors performed similarly to the ranges of 910nm - 970nm. The proposed work using GEFE achieved 61% TAR at 1% FAR, while the FEs on the 910, 911, and 970 nm spectral bands achieved 48%, 60%, and 62% TAR respectively at 1% FAR.

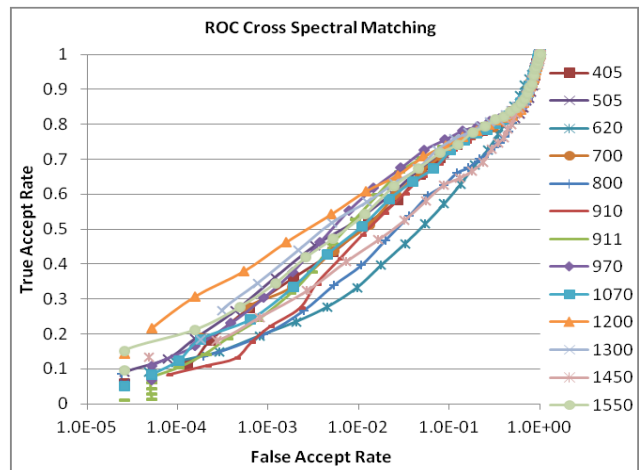


Figure 7: ROC Curves for Cross-Spectral Matching

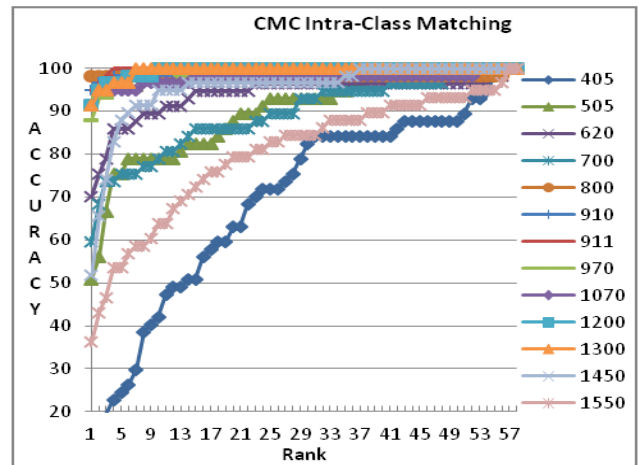


Figure 8: CMC Curves for Intra-Class Matching

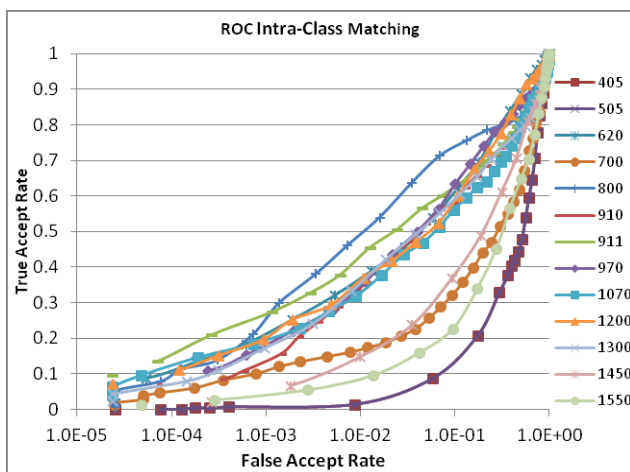


Figure 6: ROC Curves for Intra-Spectral Matching

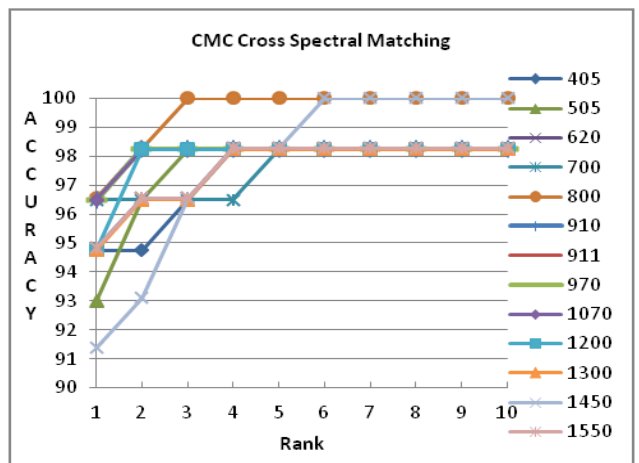


Figure 9: CMC Curves for Cross Spectral Matching.

Conclusion and Future Work

We find from the experimental results that GEFE outperforms the LBP approach for cross spectral and intra-spectral analysis. The best performing wavelength for the entire dataset was the 800nm wavelength for recognition accuracy. However, there seems to be promise with feature extractors evolved on the 1200 nm wavelength images.

Future work will be focused on fusing the cross spectral data in order to evolve features across several different spectral bands. This may improve accuracy by extracting features that may not have been present within a single spectrum.

Acknowledgements

This research was funded by the Army Research Laboratory (ARL) for the multi-university, Center for Advanced Studies in Identity Sciences (CASIS) and by the National Science Foundation (NSF), Science & Technology Center: Bio/Computational Evolution in Action Consortium (BEACON). The authors would like to thank the ARL, NSF, and BEACON for their support of this research.

References

- Adam, H., Neven, H., and Steffens, J. B. 2010. Image base multi-biometric system and method. U.S. Patent No. US7697735.
- Ahmad, F., Roy, K., and Popplewell, K. 2014. Multispectral Iris Recognition Using Patch Based Game Theory. Proc. in International Conference on Image Analysis and Recognition. pp. 112-119.
- Ahonen, T., Hadid, A., and Pietikainen, M. 2006. Face description with local binary patterns: Application to face recognition. *IEEE Transactions on Pattern Analysis and Machine Intelligence*, vol. 28, no. 12, pp. 2037-2041.
- Archbold Memorial Hospital Implements RightPatient® Patient Safety and Data Integrity System. M2SYS. N.p., 1 July 2014. Web. 11 Nov. 2014.
- Bowyer, K. W., Hollingsworth, K., and Flynn, P. J. 2008. Image understanding for iris biometrics: a survey. *Computer Vision and Image Understanding*, vol. 110, no. 2, pp. 281-307.
- Daugman, J. 2004. How iris recognition works. *IEEE Transactions on Circuits and Systems for Video Technology*, vol. 14, no. 1, pp. 21-30.
- Davis, L., ed. 1991. *Handbook of genetic algorithms*. vol. 115. New York: Van Nostrand Reinhold
- Dozier, G.V. Jan 12, 2015. Center for Advanced Studies in Identity Sciences (CASIS) Presentation.
- Engelbrecht, A.P. 2007. *Computational Intelligence: An Introduction*. John Wiley & Sons.
- Goldberg, D. 1989. *Genetic Algorithms in Search, Optimization & Machine Learning*. Addison-Wesley, Reading.
- Kennedy, J., and Eberhart, R. 1995. Particle Swarm Optimization. *Proceedings in International Conference on Neural Networks*. pp. 1942-1948.
- Masek, L. 2003. Recognition of human iris patterns for biometric identification. Dissertation B.Sc. thesis, University of Western Australia.
- Multispectral Iris Dataset: Portions of the research in this paper use the Consolidated Multispectral Iris Dataset of iris images collected under the Consolidated Multispectral Iris Dataset Program, sponsored by the US Government.
- O'Connor, B., Roy, K., Shelton, J., and Dozier, G. 2014. Iris Recognition using fuzzy level set and GEFE. *International Journal of Machine Learning and Computing (IJMLC)*, vol. 4, no. 3, pp. 225 – 231.
- Ojala, T., Pietikainen, M., and Maenpaa, T. 2002. Multiresolution gray-scale and rotation invariant texture classification with local binary patterns. *IEEE Transactions on Pattern Analysis and Machine Intelligence*, vol. 24, no. 7, pp. 971-98.
- Park, J. H., and Kang, M. G. 2005. Iris recognition against counterfeit attack using gradient based fusion of multi-spectral images. *Advances in Biometric Person Authentication*, vol. 3781, pp. 150-156.
- Popplewell, K., Roy, K., Ahmad, F., and Shelton, J. 2014. Multispectral Iris Recognition Utilizing Hough Transform and Modified LBP. Proc. in IEEE Conference on Systems, Man and Cybernetics (SMC), pp. 1396-1399.
- Ross, A. 2010. Iris recognition: The path forward. *Computer*, vol. 43, no. 2, pp. 30-35.
- Ricker, N. Penobscot County Jail Iris Scanner to Eliminate Improper Inmate Releases. *Bangor Daily News RSS*. N.p., 6 Dec. 2006. Web. 11 Nov.
- Sanchez-Avila, C., and Sanchez-Reillo, R. 2005. Two different approaches for iris recognition using Gabor filters and multiscale zero-crossing representation. *Pattern Recognition*, vol. 38, no. 2. pp. 231-240.
- Shelton, J., Dozier, G. V., Bryant, K., Small, L., Adams, J., Leflore, D., Alford, A., Woodard, D. L., and Ricanek, K. 2011. Genetic and Evolutionary Feature Extraction via X-TOOLSS. *Proceedings in International Conference on Genetic and Evolutionary Methods*.
- Shelton, J., Roy, K., O'Connor, B., and Dozier, G. V. 2014. Mitigating Iris-Based Replay Attacks. *International Journal of Machine Learning and Computing (IJMLC)*, vol. 4, no. 3, pp. 204 – 209.
- Shelton, J., Alford, A., Small, L., Leflore, D., Williams, J., Adams, J., Dozier, G. V., Bryant, K., Abegaz, T., and Ricanek, K. 2012. Genetic & evolutionary biometrics: feature extraction from a machine learning perspective. *Proceedings in IEEE Southeastcon*, pp. 1-7.
- Verma, P., Dubey, M., Verma, P., and Basu, S. 2012. Daughman's Algorithm Method For Iris Recognition- A Biometric Approach. *International Journal of Emerging Technology and Advanced Engineering*, vol. 2, no. 6, pp. 177-185.